A LIQUID CONTACT THERMAL SWITCH WITH ELECTROWETTING ACTUATION

Aric R. McLanahan, A. Hamdan, C. Richards, R. Richards
Mechanical and Material Science, Washington State University, Pullman, USA

Abstract: Recent work devoted to the development of active MEMS thermal switches is profiled. The thermal switch utilized EWOD actuation to make and break thermally conductive paths within the switch by changing the physical configuration of liquid droplets. Dynamic measurements are made to characterize the dynamic response of the switch and are compared with a simple model. Steady state thermal measurements are made to characterize the thermal resistance of the switch and are compared with a thermal resistance network. Droplet speeds of up to 2 mm/s are obtained using DI water, and thermal resistance ratios >30 are obtained using glycerin droplets under vacuum conditions.

Keywords: Thermal Switch, EWOD, MEMS

INTRODUCTION

Many proposed micro-power devices require effective thermal management. In particular, waste heat rejection from heat engines and fuel cells is of prime consideration. In order to meet these demands, the development of micro-thermal management strategies is of prime interest. Significant effort has focused on the development of active thermal switches to meet this need [1,2,3]. In the present work, the theory, fabrication, and demonstration of one such strategy, namely the use of a liquid contact micro-thermal switch, is set forth.

The thermal switch, shown schematically in Fig. 1, operates by manipulating thermally conductive paths, i.e. dielectric droplets, by changing their physical configuration on a set of silicon membranes. In the on state, heat flow directly through the liquid droplet interface. When the droplet is in the off state, heat must either flow through an air gap, or through a series of high-thermal resistance membranes to reach the other side of the switch. Using this scheme, significantly high thermal resistance ratios can be obtained.

To change the configuration of these droplets, electrowetting on a dielectric (EWOD) is employed. EWOD has already proven to be an efficient and low power actuation method on the micro scale [4]. It operates by the local modification of surface tension through an applied electric field. This produces a net electromechanical force which tends to pull the droplet further into the electric field. Linear actuation speeds of 3.3 cm/s have been reported [5]. For this switch, two sets of electrodes are fabricated across the membranes. By applying a potential between each set of electrodes, the droplet can be actuated across the membranes and into its off and on configuration.

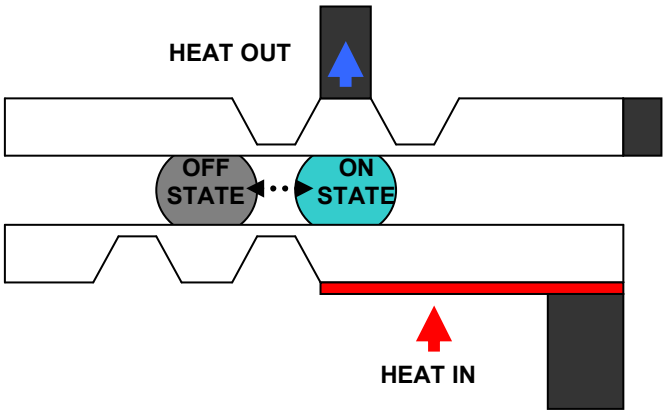

Fig. 1: Schematic of proposed thermal switch.

To characterize the switch, dynamic and thermal experiments were conducted. In the dynamic experiment, linear actuation speeds were recorded for glycerin and water at different voltages and decreasing gap thickness. For the thermal experiment, steady state heat transfer measurements were made for the switch using glycerin droplets at different pressures, gap thicknesses, and heat loads. These results were used to validate dynamic model and thermal resistance network approach.

DYNAMIC CHARACTERIZATION

Measurement

Droplet actuation speeds were measured for DI water and glycerin droplets moving in micro-channels formed by squeezing the droplet between two glass substrates. The gap width between the substrates was fixed at either 120 or 60 microns. An RMS voltage between 35 and 65 volts for water, and 40 and 65 volts for glycerin, was applied across the electrode adjacent to the liquid

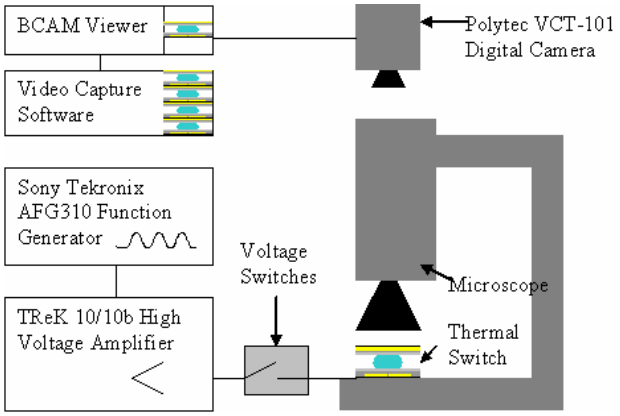

Fig. 2: Droplet actuation testing facility.

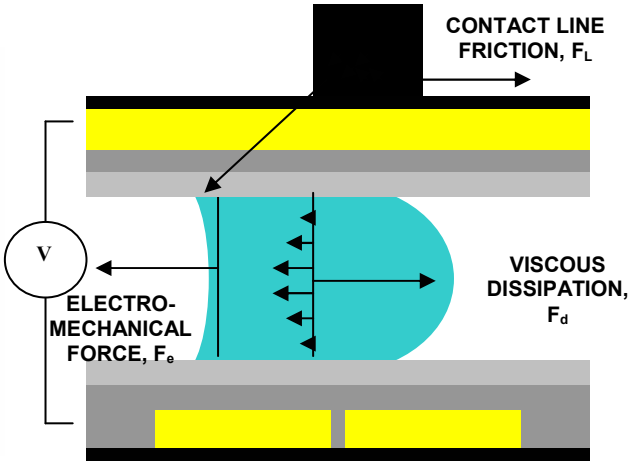

Fig. 3: Overview of main forces action on droplet.

droplet using a Sony Tekronix AFG310 function generator and a TReK 10/10b high voltage amplifier. The resulting motion of each droplet was recorded through the top transparent electrode using a Polytec VCT-101 digital camera as shown in Fig. 2. The speed of each droplet was determined by analyzing the motion of the droplet in successive images.

Modeling

Actuation of a liquid droplet via EWOD is modeled by applying a force balance on the droplet. We consider the effect of three forces in this model: the driving force due to electrowetting, the viscous forces at the interface between the liquid droplet and the solid substrate, and the contact line friction (Fig. 3). The electrowetting driving force is modeled using the appropriate Maxwell stress tensor:

$$T^e_{mn} = \varepsilon E_m E_n - \delta \frac{1}{2} \varepsilon E_k E_k \qquad (1)$$

where T^e_{mn} is the stress tensor, E is the electrical field, ε is the permittivity, and δ is the Kronecker delta function. Two assumptions are made. Electrostriction effects are assumed negligible, and no free charge is assumed to be present. If the electrical field, E , is known, the electrowetting driving force can be obtained by taking a closed surface integral of T^e_{mn} around the volume of interest [6]. Obtaining an analytical solution for the electric field at the interface of the droplet is difficult. However, far away from the interface, where the electric field is uniform, the integral can be found from a circuit diagram. The driving force per unit length is then modeled as

$$F_e = \sum_{i=1}^{n} \frac{\varepsilon E_i^{\,2} d_i}{2} - \sum_{j=1}^{n} \frac{\varepsilon E_k^{\,2} d_k}{2} \qquad (2)$$

where E_i is the magnitude of the electric field through the droplet, E_k is the magnitude of the electric field through the surround vapor, and d is the respective thickness of the capacitive layers.

Retarding droplet motion is viscous dissipation. The viscous force is modeled using the Darcy-Weisbach equation:

$$F_d = f \frac{\rho U^2}{8} A_c \qquad (3)$$

where f is the Darcy friction factor, U is the velocity, and A_c is the cross sectional area [7].

The force due to contact line friction, caused by molecules at the contact line sliding past each other, also oppose motion, and scale with velocity:

$$F_L = \zeta U \qquad (4)$$

Here ζ is a contact line friction coefficient, which is a function of the surface roughness.

The average velocity of a droplet is determined by setting the sum of forces acting on the droplet equal to zero.

$$F_e - F_d - F_L = 0 \qquad (5)$$

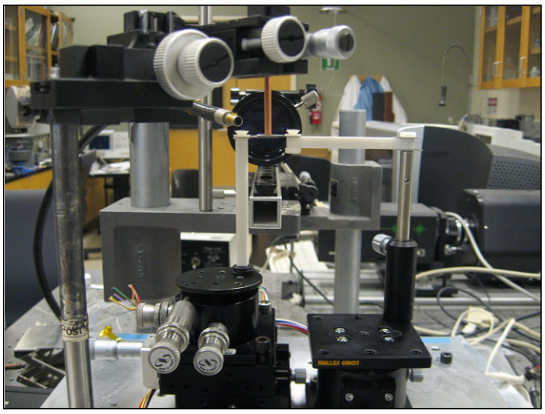

Fig. 4: Thermal characterization test facility

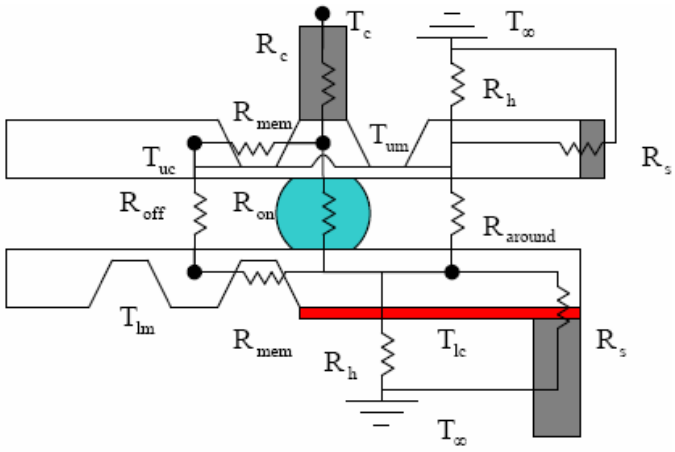

Fig. 5: Thermal resistance network in the on state.

THERMAL CHARACTERIZATION

Measurement

A prototype thermal switch was fabricated using standard silicon micro-machining technology. To thermally characterize the switch, an experimental test facility was constructed (Fig. 4). Two 6.4x6.4 mm thick, 76 mm long ceramic support beams were used to rigidly support the two die making up the thermal switch. Three sets of Melles Griot stages allowed precise positioning of the die. An Infinity K2/SC long distance microscope was used to visualize, align, and space the die. Heat transfer into the switch was accomplished by a resistance heater glued to the bottom of thermal switch die. Temperatures were measured across the switch using PRTs coupled to a Wheatstone bridge.

A 25 mm copper "cold finger" made contact with the top of the thermal switch to provide a path for heat transfer out of the switch. A Welch Series 3 vacuum pump was used to reduce pressure in the test facility as low as 0.55 Torr.

The thermal characterization of the switch consisted of a set of measurements of heat transfer across the switch. A glycerin droplet was used for the liquid droplet. Measurements were made for three gap thicknesses: 120, 60, and 30 microns and at four gap pressures: atmospheric pressure and 10, 1, and 0.57 Torr. For each condition, five increasing heat loads were applied to the switch, by dissipating electrical power in the resistance heater on the bottom switch die. The temperature difference across the switch, as well as the electrical power dissipated in the resistance heater, were then recorded. The thermal resistance of the switch was taken to be the heat transfer rate through the switch to the cold finger divided by the temperature difference across the switch. Because energy was lost to the switch surroundings through natural convection and radiation, not all of the heat generated at the base of the switch ended up going through the switch to the cold finger. To determine the difference, the thermal resistances of the switch without the cold finger were also measured to determine this magnitude. This allowed for the actual amount of heat traveling through the cold finger in the off and on states to be determined.

Modeling

Heat transfer rates across the thermal switch were predicted using a 2D thermal resistance network. Fig. 5 shows the thermal resistance network for the device "On" state. The temperatures for each isothermal region in the device were determined by imposing energy conservation and

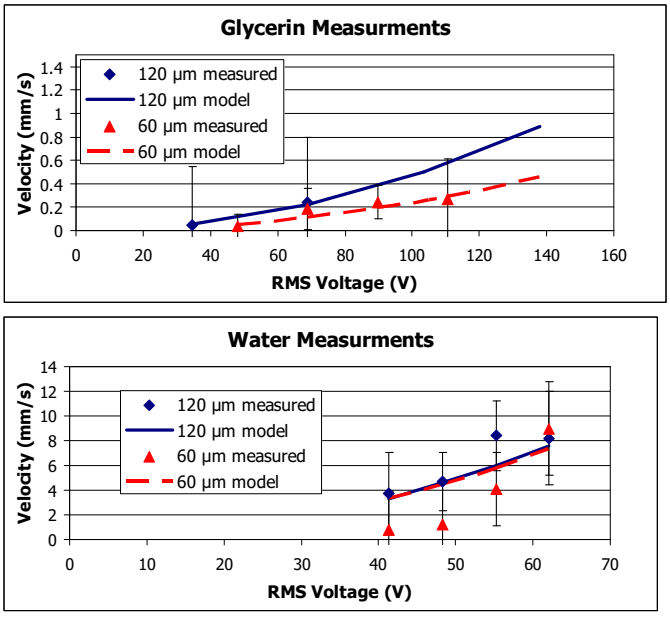

Fig. 6: Results of dynamic measurement and model. .

Table 1: Results of thermal measurements at 30 µm.

	Pressure (Torr)	$R_{measured}$ (K/W)	$\pm U_r$ (K/W)	Rmodeled (K/W)
off	760	21.2	10.7	24.5
	10	41.5	9.7	36.7
	1	63.5	10.3	61.5
	0.57	72.1	9.9	69.4
on	760	6.3	2.2	6.1
	10	6.0	2.7	5.5
	1	5.6	2.3	5.3
	0.57	5.4	2.2	5.6

solving for heat transfer through each conductive path iteratively. Heat transfer rates were determined using these temperatures and the known thermal resistances in the network.

RESULTS

Dynamic results of both the modeling and experimental efforts are given in Fig. 6. Droplet speeds between 0.8 - 9 mm/s were measured for DI water, and 0.4-0.27 mm/s for glycerin. These actuation speeds imply device switching speeds of 15 - 22 seconds for a thermal switch based on a glycerin droplet travel distance of 6 mm.

Heat transfer results for the thermal switch using a glycerin droplet in a 30 microns thick gap are shown in Table 1. As the pressure decreases, the thermal resistance in the off state increases while the thermal resistance in the on state remains nearly constant. Measurements of the thermal resistance are seen to agree with the predictions of the 2D model and are within the experimental uncertainty for all cases.

Table 2 shows measured and modeled thermal resistance ratios R_{off}/R_{on} for the 30 micron gap switch at decreasing pressures. These thermal resistance ratios were calculated by considering only the amount of heat traveling through the cold finger, and not the energy lost to the environment through radiation and convection. As the operating pressure drops, the measured thermal resistance ratio is seen to increase from 6.5 to 32.7.

Table 2: Actual thermal resistance ratios at 30 µm

Pressure (Torr)	Measured $R_{off/on}$	Modeled $R_{off/on}$
760	6.5	8.6
10	11.5	12.4
1	27.0	30.9
0.57	32.7	40.4

DISCUSSION

The design, fabrication, and characterization of a MEMS thermal switch have been presented. The thermal switch operates by changing the conductive path between two silicon die by moving a dielectric liquid, glycerin, using electrowetting. The result is a bi-stable thermal switch that can change between a low thermal resistance state and a high thermal resistance state. Preliminary measurements show the switching time on the order of 30 seconds. Measured thermal resistances ratios of $R_{off/on} > 30$ have been demonstrated for a thermal switch employing a glycerin droplet actuated in a 30 micron thick gap, operating at a pressure of 0.57 Torr.

REFERENCES

[1] Cho J, Richards C, Bahr D, Jiao J, Richards R 2008 Evaluation of contacts for a MEMS thermal switch *J. Micromech. Microeng,* **18** 105012

[2] Cho J, Wiser T, Richards C, Bahr D, Richards R. 2007 Fabrication and characterization of a thermal switch *Sens. Act.: A. Physica.* **133** 55-63

[3] Tsukamoto T., Esahi M., Tanaka S. 2009 Long working range mercury droplet actuation J. *Micromech. Microeng* **19** 094016

[4] Moon H., Cho S., Garrell R., Kim C. 2002 Low Voltage electrowetting-on-dielectric, *J. of Applied Physics*, **92**

[5] Sen P, Kim C. 2005 Electrostatic fringe-field actuation for liquid-metal droplets *Transducers 05' International Conference* 705-708

[6] Jones T, Fowler J, Chang Y, Kim CJ 2003 Frequency-based relationship of electrowetting and dielectrophorectic liquid microactuation *Langmuir* **19** 7646-7651

[7] Steinke M, Kandlikar S, 2006 Single-phase liquid friction factors in microchannels *International Journal of Thermal Science* **45** 1073-1083